Data Paper

The International Journal of Robotics Research
2017, Vol. 36(12) 1247–1251

DOI: 10.1177/0278364917732838
journals.sagepub.com/home/ijr

Underwater caves sonar data set

Angelos Mallios, Eduard Vidal, Ricard Campos and Marc Carreras

Abstract

This paper describes a data set collected with an autonomous underwater vehicle testbed in the unstructured environment of an underwater cave complex. The vehicle is equipped with two mechanically scanned imaging sonar sensors to simultaneously map the caves horizontal and vertical surfaces, a Doppler velocity log, two inertial measurement units, a depth sensor, and a vertically mounted camera imaging the sea floor for ground truth validation at specific points. The testbed collected the data in July 2013, guided by a human diver, to sidestep autonomous navigation in a complex environment. For ease of use, the original robot operating system bag files are provided together with a version combining imagery and human-readable text files for processing on other environments.

Keywords

Underwater robotics, acoustic imaging sonar, simultaneous localization and mapping, underwater caves, field and service robotics

1. Introduction

Most autonomous underwater vehicle (AUV) operations are conducted in open water and where the seafloor is relatively smooth with limited obstacles, providing adequate safety margins for the vehicle's navigation drift error. However, confined environments compose a large application space (oil & gas, search & rescue, science, etc.) that is inadequately served by remotely operated vehicles and divers. Although it is an important area of study, there is limited published research on simultaneous localization and mapping (SLAM) in confined underwater environments, mostly because of the inherent difficulties for conducting experiments.

This paper presents a data set collected with an AUV testbed from an experiment conducted in the unstructured environment of an underwater cave complex. The survey was performed in July 2013 with the aim of demonstrating the feasibility of localizing an AUV in that challenging setting without the need for external navigation aids, and to collect data for further research in autonomous underwater navigation. To ensure the AUV's safety and the collection of a complete dataset in a limited time, the vehicle was guided by a diver throughout the caves. The vehicle path trajectory has been designed to contain several loop closures, which should be useful for testing SLAM algorithms. The data set is available for download from our server at http://cirs.udg.edu/caves-dataset/. Readers can find an example use of this data set and a reference for comparison of their own results in Mallios et al. (2015).

To the best of our knowledge, this data set is the first of its kind that is publicly available, and it is our hope that the data paper will be useful for other researchers in the area of autonomous exploration in confined underwater environments.

2. Sensors

An early version of the *Sparus* AUV series (Carreras et al., 2015) was used as a testbed for this experiment. Due to the vehicle's limited payload area, it was modified to carry the following navigation and perception sensor suite. Table 1 presents the specifications of the sensors used to generate this data set.

2.1. Navigation sensors

1. Xsens MTi (XSens, 2010) is a low cost attitude and heading reference system (AHRS) based on a microelectromechanical system (MEMS), integrating

Universitat de Girona, Girona, Spain

Corresponding author:
Angelos Mallios, Computer Vision and Robotics Institute (VICOROB), Carrer Pic de Peguera 13, Parc científic i tecnològic, Edifici CIRS, Girona 17003, Spain
Email: amallios@eia.udg.edu

3D gyroscopes, accelerometers, and magnetometers. Its onboard processor unit runs a proprietary fusion algorithm providing real-time estimates of attitude, heading and inertial dynamic. The MTi is the standard AHRS of the early *Sparus* AUV and is located inside the vehicle's electronics pressure housing.

2. Analog Devices ADIS16480 (Analog Devices, 2013) is a 10 degrees of freedom MEMS inertial sensor with dynamic orientation outputs. It also includes a triaxial gyroscope, a triaxial accelerometer, and a triaxial magnetometer, fused with an extended Kalman filter (EKF) for dynamic orientation sensing. This sensor was installed in a separate pressure housing and outside of the vehicle's hull to minimize electromagnetic interference from the vehicle.
3. LinkQuest NavQuest 600 Micro (LinkQuest, 2012) is a Doppler velocity log (DVL) sensor that provides 3D vehicle velocities with respect to the seafloor or a water layer. Integration of these velocities with AHRS measurements is a common technique to reduce dead-reckoning drift on underwater vehicle navigation.

2.2. Perception sensors

1. Tritech Micron DST (Tritech, 2010a) is a compact mechanically scanned imaging sonar (MSIS) commonly used for obstacle avoidance on remotely operated vehicles (ROVs). Its operating frequency is chirped from 650 kHz to 750 kHz with a beamwidth of 35 deg vertical by 3 deg horizontal. In this experiment the DST is used to sense the cave walls on the horizontal plane with the following settings: continuous 360 deg scan sector on 200 steps at 50 m range. Each beam provides intensity measurements every 0.126 m (397 bins).
2. Tritech Super SeaKing DFP (Tritech, 2010b) is a dual frequency profiling sonar most commonly used in constructions applications. Its two operating frequencies are 0.6 MHz and 1.1 MHz with a conical beamwidth of 2 deg and 1 deg respectively. In this experiment the sensor is used to scan the cave walls on the vertical plane with the following settings: continuous 360 deg scan sector on 200 steps at 1.1 MHz frequency and 20 m range. The sonar is configured in imaging mode and each beam provides intensity measurements every 0.4 m (50 bins).
3. Finally, a low cost analog video camera (PAL) was mounted looking down in order to identify ground truth features (see Section 3.1). The vehicle's architecture was capturing still frames from the video feed at 4 Hz.

Table 1. Summary of the sensor suite specifications.

System	Specifications
Testbed - *Sparus* AUV	
Depth rated	50 m
Size	1.22(L) $\times$0.23(D) m
Mass	25 kg
Energy	890 Wh
DVL - LinkQuest NavQuest 600 Micro	
Frequency	600 kHz
Velocity accuracy	0.2 % $\pm$1 mm/s
Altitude	0.3 – 140 m
Max ping rate	5 Hz
AHRS - Analog Devices ADIS16480	
Static accuracy (roll/pitch)	0.1 deg
Static accuracy (Heading)	0.3 deg
Dynamic accuracy (roll/pitch)	0.3 deg
Dynamic accuracy (Heading)	0.5 deg
AHRS - XSens MTi	
Angular resolution	0.05 deg
Repeatability	0.2 deg
Static accuracy (roll/pitch)	0.5 deg
Static accuracy (Heading)	1 deg
Dynamic accuracy	2 deg RMS
Depth - DS2806 HPS-A	
Pressure range	0 – 5 bar
Output span	4V $\pm$1%
Output zero	1V $\pm$1% of span
Repeatability	$\pm$0.25 % of span
Imaging sonar - Tritech Micron DST	
Frequency	Chirped 650 to 750 kHz
Max range	75 m
Horizontal beamwidth	3 deg
Vertical beamwidth	35 deg
Scan rate (360 deg sector)	5 $-$ 20 sec
Profiling sonar - Tritech Super SeaKing DFP	
Frequency	0.6 | 1.1 MHz
Max range	80 | 40 m
Beamwidth	2 | 1 deg
Scan rate (360 deg sector)	4 $-$ 25 sec
Down-looking analog camera	
System	PAL
Resolution	384 $\times$ 288 pixels
Lighting source	2 $\times$ 24 W HID

2.3. Sensors offsets

The perceptual and navigation sensors are fixed to the vehicle and can be related with rigid-body transformations. The reference frame of the DVL has been defined as the body frame of the vehicle and all other coordinate frames are defined with respect to it (Figure 1). In Table 2 these transformations are provided with respect to the body frame.

All measurements have been obtained manually and, for practical purposes, the uncertainty can be considered to be $\pm$2 cm.

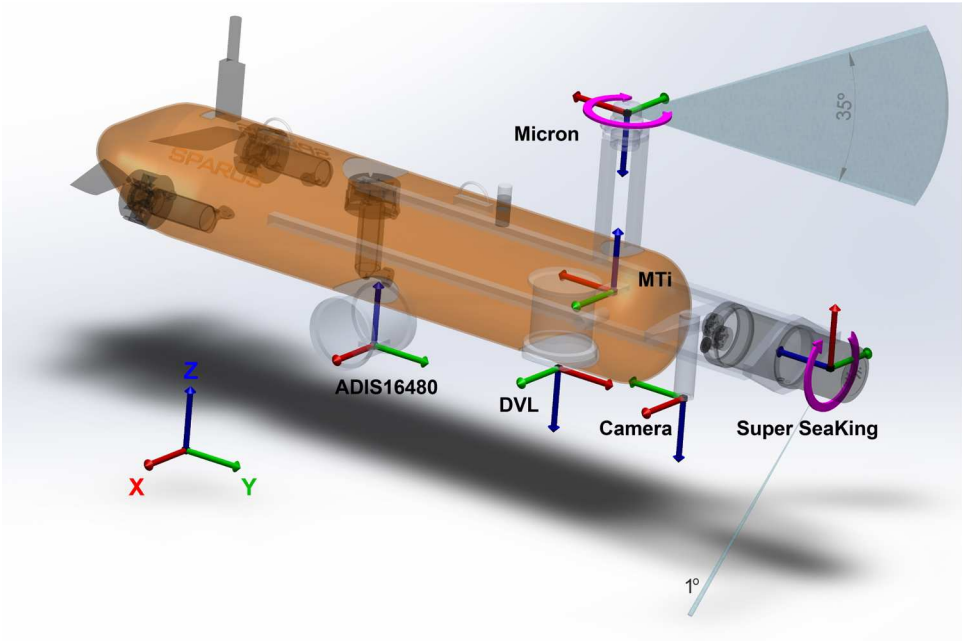

Fig. 1. Relative position of the sensor frames with respect to the DVL frame (i.e. the body frame).

Fig. 2. Approximate positions of cones and paths traveled underwater, overlaid on an aerial image from Google Earth.

3. Data set overview

The data set was obtained in the underwater cave complex "Coves de Cala Viuda", located in the L' Escala area of Costa Brava, Spain (Lat: 42.103883 N, Lon: 3.182550 E) (Figure 2). The complex consists of three single-branch caves and several tunnels of different sizes and is part of a broader cave complex in the area that is popular among recreational divers (Llamas and Cáceres, 2010). This data set explores two of the caves and tunnels, closing a loop approximately 500 m long. The floor of the cave entrance is approximately 20 m deep and ascends, following corridors with diameters varying from 1 m to 17 m, to interior surface air chambers at the end of each cave.

Table 2. Sensor offsets.

Sensor	Value (meters and degrees) [x, y, z, roll, pitch, yaw]
DVL	[0.00, 0.00, 0.00, 0°, 0°, 0°]
ADIS16480	[–0.38, 0.00, 0.07, 180°, 0°, 90°]
MTi	[0.10, 0.00, –0.16, 180°, 0°, –90°]
Pressure	[–0.06, 0.00, –0.10, 0°, 0°, 0°]
Micron	[0.10, 0.00, –0.42, 0°, 0°, 180°]
Super SeaKing	[0.55, 0.00, –0.15, 0°, 90°, 180°]
Camera	[0.26, 0.00, –0.02, 0°, 0°, 90°]

3.1. Ground truth

In natural overhead underwater environments, it is not trivial to obtain absolute ground truth. Our approach is to support this data set with ground truth points for relative accuracy estimation. For validation of the algorithm, the data set includes six traffic cones as ground truth points that can be easily distinguished on the images (Figure 3). The cones were placed in strategic locations along the AUV trajectory which the vehicle passed over twice, closing loops, including the entrances of the caves and the beginning and end of the survey.

The relative position of the cones can be found by extracting the timestamps from the video frames where the cones appear closest to the center of the image, and compare them with the timestamps of the trajectory. The relative displacement between the cone and the reference frame of the vehicle can then be found by using the existing camera calibration (Bouguet, 2004). A simple measure of the displacement in the X-Y plane can be computed by assuming a planar seafloor, orthogonal to the viewing direction

Table 3. Cone pairs distance (*see text about ground truth accuracy).

Cone pairs	Distance (m)*
1 - 2	19
2 - 3	32
3 - 4	16
1 - 6	30

Fig. 3. One of the cones used as a ground truth point.

of the camera. Having the measures of the cone base (20x20 cm), one can directly compute the metric resolution of a pixel, and convert the displacement in pixels to meters. More complex measures could involve using the planar base of the cone as the input into the Direct Linear Transform method to compute the camera pose (Hartley and Zisserman, 2004).

An additional ground truth step was included by manually measuring the distances between the cones with a tape measure (Table 3). Due to long distances and rock outcrops between the cones, the measuring tape did not always follow a straight line, so these measurements represent an upper bound of unknown variance. These tape measurements can help bound the scaling error (a problem which is very common with scan matching algorithms in corridor areas) by providing a maximum length scale.

On the vertical plane, displacements are well instrumented and recorded with absolute measurements from the pressure sensor with centimeter accuracy. The very low tidal variability of the area, which is comparable to the pressure sensor uncertainty, and the relatively short duration of the experiment suggest that pressure data can be considered accurate compared to horizontal displacement measurements.

3.2. Data structure

Data from all sensors was stored asynchronously using robot operating system (ROS) (ROS, 2013). The ROS framework provides a standardized and straightforward way to playback the individual log files and visualize the data. To ease data set usage, a standard dead-reckoning EKF based model is provided for quick visualization of the trajectory and data. A human readable version of the logs and images is also provided in standard format to support long-term data archival, and for researchers that prefer to use other tools.

3.2.1. ROS bag files. At the time of the experiment raw sensor data was collected using robot operating system (ROS) Fuerte. However, data is provided as updated ROS Jade bag files. A ROS package (named *cirs_girona_cala_viuda*) containing required messages and useful scripts to visualize the data is also provided.

The main bag file contains the following topics.

1. */depth_sensor*: DS2806 HPS-A pressure sensor data.
2. */dvl_linkquest*: LinkQuest NavQuest 600 sensor data. Contains bottom and water referenced velocities and raw sensor data.
3. */imu_adis*: Analog Devices ADIS16480 sensor data. Contains orientation as both Euler angles and quaternions. It also contains raw data for accelerometers, gyros, magnetometers and temperature, and an estimate of the gyro biases.
4. */imu_adis_ros*: Analog Devices ADIS16480 sensor orientation using a standard IMU ROS message.
5. */imu_xsens_mti*: Xsens MTi sensor data. Same message type as the topic */imu_adis*.
6. */imu_xsens_mti_ros*: Xsens MTi sensor orientation using a standard IMU ROS message.
7. */odometry*: estimation of the robot pose provided as a standard *Odometry* ROS message.
8. */sonar_micron*: Tritech Micron DST sensor beam data.
9. */sonar_micron_ros*: micron data provided as a standard *Laserscan* ROS message.
10. */sonar_seaking*: Tritech Super SeaKing DFP profiler sensor beam data.
11. */sonar_seaking_ros*: profiler data provided as a standard *Laserscan* ROS message.
12. */tf*: standard ROS messages containing sensor offsets described in Section 2.3.

The optical data represents the largest part of the data set size. However, depending on the application, optical data may not be required. For this reason, separate bag files storing the optical data alone are provided. These data include images, in typical ROS raw format (*/raw_image* topic), camera calibration (*/camera_info* topic), and */tf* messages containing offsets for the camera sensor (i.e. last row of Table 2). The camera model follows Bouguet (2004). Camera parameters are those described in the standard */camera_info* topic. For reference, the following list describes the set of relevant parameters:

- width/height: the image's width and height in pixels;
- distortion_model: the distortion model assumed, which in this case is the "plumb bob" model (Brown, 1966);

- D: the five distortion coefficients of the distortion model presented above;
- K: 3 × 3 pinhole model calibration matrix.

Note parameters in the standard camera_info message that only relate to stereo camera configurations are omitted (meaningless for the monocular configuration used in this experiment) or to regions of interest within the image. Moreover, it is worth noting that camera calibration was not performed on site, but in a fresh water tank after the experiments. Due to operational difficulties, it was not possible to collect calibration data on site, in seawater. However, the calibration performed on the water tank provides a good approximation that considers the refraction effects of the water medium.

3.2.2. Text files. Text files containing the same data as the bag files are also included. They have been formatted as *comma-separated values* files, and the first line of each file contains a header with the description of the data represented in each column. There is a text file for each topic in the bag file.

3.2.3. Images. The images contained in the bag file have been extracted for ease of use by a non-ROS user in two modalities. First, we provide the original color images following the naming convention: "frame_<frame_number>.png". An accompanying text file relates each of the file names to its corresponding time stamp. In addition, the undistorted version of the previous images are extracted using the distortion parameters in the bag files. In this case, the naming convention of the image files is "frame_ud_<frame_number>.png". We also provide a text file relating the image name with its time stamp. Finally, in order to allow the reproduction of the camera calibration, the full data set of calibration images collected in the water tank is also contained in the bag files.

4. Summary

We have presented a data set collected with an autonomous underwater vehicle testbed in the unstructured environment of an underwater cave complex. The vehicle trajectory has been designed to contain several loop closures, which should be useful for testing various SLAM algorithms. It is our hope that the data paper will be useful to other researchers in the area of autonomous exploration in confined underwater environments. The data set is available for download from our server at http://cirs.udg.edu/caves-dataset/.

Acknowledgements

The authors wish to thank Arnau Carrera and Emili Hernández for their help on the survey, as well as the members of the Computer Vision and Robotics research group at Universitat de Girona (UdG) Guillem Vallicrosa, Narcís Palomeras, and Nuno Gracias for thorough discussions on the preparation of this data set.

Funding

The author(s) disclosed receipt of the following financial support for the research, authorship, and/or publication of this article: This research has been partially supported by the EU FP7 project Techniospring-Marie Curie (TECSPR13-1-0052), and the Spanish project ARCHROV (DPI2014-57746-C3-3-R).

References

Analog Devices (2013) The ADIS16480 inertial system. Available at: http://www.analog.com/en/products/sensors/inertial-measurement-units/adis16480.html (accessed 29 November 2016).

Bouguet JY (2004) Camera calibration toolbox for Matlab. Available at: http://www.vision.caltech.edu/bouguetj/calib_doc/index.html (accessed 29 November 2016).

Brown DC (1966) Decentering distortion of lenses. *Photometric Engineering* 32(3): 444–462.

Carreras M, Candela C, Ribas D, et al. (2015) Testing SPARUS II AUV, an open platform for industrial, scientific and academic applications. In: *Instrumentation viewpoint*, volume 18. SARTI, pp. 54–55. Spain.

Hartley RI and Zisserman A (2004) *Multiple View Geometry in Computer Vision*. 2nd edition. UK: Cambridge University Press.

LinkQuest (2012) NavQuest 600 micro Doppler velocity log. Available at: http://www.link-quest.com/html/models_nq.htm (accessed 29 November 2016).

Llamas A and Cáceres P (2010) *Guía submarina de les Illes Medes i la Costa del Montgrí*. Spain: Anthias.

Mallios A, Ridao P, Ribas D, et al. (2015) Toward autonomous exploration in confined underwater environments. *Journal of Field Robotics* 33(7): 994–1012.

ROS (2013) Robot Operating System (ROS). Available at: www.ros.org.

Tritech (2010a) Micron - Mechanical Scanning Sonar. Available at: http://www.tritech.co.uk/product/small-rov-mechanical-sector-scanning-sonar-tritech-micron (accessed 29 November 2016).

Tritech (2010b) Super SeaKing DFP - Dual Frequency Profiler. Available at: http://www.tritech.co.uk/product/dual-frequency-profiler-super-seaking-dfp (accessed 29 November 2016).

XSens (2010) MTi - Miniature based AHRS. Available at: https://www.xsens.com/products/mti/ (accessed 29 November 2016).